Limnol. Oceanogr., 46(4), 2001, 802–810

Assessment of photosynthesis in a spring cyanobacterial bloom by use of a fast repetition rate fluorometer

David Suggett
Southampton Oceanography Centre, University of Southampton, Southampton, SO14 3ZH, United Kingdom

Gijsbert Kraay
NIOZ, Landsdiep 4, NL-1797 SZ, 't Horntje (Texel), The Netherlands

Patrick Holligan
Southampton Oceanography Centre, University of Southampton, Southampton, SO14 3ZH, United Kingdom

Margaret Davey
Marine Biological Association of the United Kingdom, Citadel Hill, Plymouth, PL1 2PB, United Kingdom

Jim Aiken
Plymouth Marine Laboratory, Prospect Place, Plymouth, PL1 3DH, United Kingdom

Richard Geider[1]
Marine Biological Association of the United Kingdom, Citadel Hill, Plymouth, PL1 2PB;
Department of Biological Sciences, University of Essex, Colchester CO4 3SQ, United Kingdom

Abstract

Estimates of gross primary production (GPP) based on fast repetition rate fluorometer (FRRF) measurements were compared with independent ^{14}C and O_2 at three stations during a spring bloom in the North Atlantic. A photosynthesis versus irradiance (P-E) curve was constructed for each station from the observations of in situ photon efficiency of photosynthesis. This composite P-E curve was compared with P-E curves determined for discrete samples from ^{14}C assimilation. Estimates of α^{Chl} and P_m^{Chl} from the ^{14}C-uptake method were 1.5–2.5-fold lower than those estimated from the FRRF data. Much of this discrepancy can be accounted for if ^{14}C assimilation approximates net phytoplankton photosynthesis with use of a photosynthetic quotient of 1.4 mol O_2 (mol CO_2)$^{-1}$. Photosynthetic oxygen consumption may have also contributed to the difference. In situ GPP was calculated from incident irradiance, light attenuation, light absorption by phytoplankton, and the light dependence of the in situ photon efficiency. This estimate of GPP was two times greater than net community photosynthesis determined from diel changes of in situ oxygen concentration. Thus, the in situ net O_2 and in vitro ^{14}C techniques yielded similar estimates of phytoplankton photosynthesis that were about twofold lower than the estimates of GPP provided by FRRF. Uncertainties in the FRRF technique associated with choosing an appropriate value of photosynthetic unit size and fitting a P-E curve to the in situ measurements are discussed. Despite these uncertainties, the FRRF results were consistent with the independent estimates of phytoplankton productivity.

Chlorophyll fluorescence can be used to estimate primary production by use of both ''active'' (Kolber et al. 1998) and ''passive'' (Hu and Voss 1998) methods. The fast repetition rate fluorometer (FRRF) provides measurements of the progressive closure of photosystem II (PSII) reaction centers (Sakshaug et al. 1997) in response to flashes of excitation energy and is a technological development from the earlier pump and probe (PP) technique (e.g., Kolber et al. 1998). Both methods are based on similar principles. However, the FRRF is a more flexible instrument, which gives relatively instantaneous measurements of certain physiological parameters, thus shortening the overall protocol (Sakshaug et al. 1997). In addition, the FRRF provides a better signal-to-noise ratio and allows more robust measurements in low chlorophyll regions. As such, the FRRF allows phytoplankton productivity to be examined with a spatial and temporal resolution that is unprecedented in aquatic research. The FRRF has the potential to provide more rapid and accurate measurements of productivity in natural waters by allowing the coupling of phytoplankton productivity to physical forcing to be examined on the scales of transient phenomena such as fronts or storms. These transient phenomena have a

[1] Corresponding author (geider@essex.ac.uk).

Acknowledgements

The authors wish to thank Gerald Moore (Plymouth Marine Laboratory) for his help with the collection and manipulation of spectral light data, Klaas Timmermans and Ruud Groenewegen for providing cruise hydrographic data, and the Captain and crew of RV *Pelagia* (NIOZ), March 1998. This work was supported by the European Commission through MAST project MERLIM (contract MAS3-CT95-0005) and through the NERC (grant GR3/11829).

disproportionate impact on productivity and are particularly relevant within the context of the functional responses of aquatic systems to global climate change.

A 1:1 relationship between ^{14}C measurements and FRRF estimates of carbon fixation was found by the originators of the technique (Kolber and Falkowski 1993). This result is somewhat surprising, since the FRRF measures gross electron transfer rate (ETR), which should be related to gross photosynthesis, whereas ^{14}C is commonly assumed to measure net carbon fixation (Williams et al. 1996). A recent study by Boyd et al. (1997) found that PP technique underestimated ^{14}C productivity by a factor of ~1.5. There are numerous reasons why FRRF and ^{14}C methods should not give identical results. These include differences in sample treatment (in situ versus in vitro incubations), differences in currency (ETRs vs. carbon assimilation), and a number of methodological problems with both techniques. The key assumptions and uncertainties in the FRRF technique, as it is applied to the study of natural phytoplankton populations, have not been rigorously assessed.

Estimation of the rate of photosynthesis—The principles governing the application of the FRRF for studies of marine phytoplankton production are described by Falkowski and Raven (1997). Here we summarize the estimation of production from PP (Kolber and Falkowski 1993; Falkowski and Kolber 1995; Boyd et al. 1997) and FRRF (Babin et al. 1996; Falkowski and Raven 1997; Sakshaug et al. 1997) methodologies as the basis for a rigorous direct comparison of production measurements that use FRRF, in vitro ^{14}C assimilation, and in situ diel O_2 techniques in the Atlantic Ocean.

The fluorescence yield (or efficiency) is a quantitative measure of fluorescence from PSII and is defined as the ratio of photons emitted to photons absorbed. The oxygen yield is the ratio of O_2 evolved to photons absorbed by PSII. Both fluorescence and oxygen yields are the result of reactions that occur in PSII (Falkowski and Raven 1997), and the action spectra for these two processes are remarkably similar. Measurements made by FRRF can be used to estimate gross photosynthetic oxygen evolution from the following photosynthetic model (Kolber and Falkowski 1993):

$$P^{\mathrm{RCII}}(E) = E\,\sigma_{\mathrm{PSII}}\,qP(E)\,\phi_e(E)\,f, \quad (1)$$

where $P^{\mathrm{RCII}}(E)$ is the oxygen evolution rate (μmol O_2 photon^{-1} s^{-1}), E is the irradiance (μmol photons m^{-2} s^{-1}), σ_{PSII} is the photochemically effective cross-section for PSII (m^2 photon^{-1}), qP is the photochemical quenching coefficient (dimensionless and always $\leq$1.0) under ambient light, and ϕ_e is the photon yield of electron transfer by PSII (mol O_2 mol photon^{-1}). f is the proportion of PSII reaction centers that are functional (dimensionless) and is directly related to the variable fluorescence yield, F_v (*see Methods*).

Modification of Eq. 1 to take account of the relationship between oxygen produced and carbon fixed and the concentration of RCII reaction centers per unit volume gives photosynthetic carbon fixation per unit volume:

$$P_z = (E_z\,\sigma_{\mathrm{PSII}}\,qP\phi_e\,f\,n_{\mathrm{PSII}}\,[\mathrm{Chl}\ a]\ 2.43 \times 10^{15})/PQ, \quad (2)$$

where P_z is the photosynthetic carbon fixation per unit volume of seawater at depth z (mol CO_2 m^{-3} h^{-1}), n_{PSII} is the ratio of RCII to chlorophyll a (mol photon [mol Chl a]$^{-1}$), PQ is the photosynthetic quotient (mol O_2 evolved [mol CO_2 incorporated]$^{-1}$), [Chl a] is the Chl a concentration (mg m^{-3}), and 2.43×10^{15} is a numerical factor to account for the conversion of seconds to hours, photons to moles of reaction centers, mol Chl a to mg Chl a, and μmol O_2 to mol O_2. All other parameters are defined as in Eq. 1 but with reference to depth z. As for n_{PSII}, values for PQ must be assumed or estimated by other methods. For convenience, the PQ is assumed to be 1.0 for FRRF estimations of production unless stated otherwise.

Methods

Sampling on the Merlim98 cruise of RV *Pelagia* (cruise 64 PE 114) in March 1998 was undertaken at three sites along the 23°W meridian: Sta. 1 at 43°N (13–14.3.98), Sta. 2 at 40°N (16–17.3.98), and Sta. 3 at 37°N (18–19.3.98). At each site, a series of conductivity temperature depth (CTD) casts (a minimum of seven per site) was made over a 24-h period starting at 0800 h GMT (0700 h local time). Sky conditions throughout the diel sampling period remained overcast at Sta. 1 but were predominantly free from clouds at Sta. 2 and 3.

CTD instrument package—A SeaBird 9+ CTD was equipped with pressure, conductivity, temperature, and polarographic oxygen sensors. Also attached to the CTD frame were a SeaTech 25-cm path length transmissometer (at 660 nm), a NIOZ cosine light sensor (550 nm), a set of Technicap water samplers (10.3-liter capacity), and a Chelsea Instruments (CI) FAST*tracka* titanium FRRF (serial number 182018) with a 2π collector CI photosynthetically available radiation (PAR) (400–700 nm) sensor. The FRRF was mounted onto the CTD frame in place of one of the water bottles. The CTD light and FRRF photosynthetically available radiation (PAR) sensors were at the same height and gave comparable outputs ($r^2 > 0.97$). The PAR sensors measure the photon flux density between 400 and 700 nm, herein subsequently referred to as ''irradiance.''

The FRRF was configured with both a light chamber and a dark chamber in which the phytoplankton are retained in the dark long enough to allow relaxation of the variable fluorescence yield (F_v) (the maximum fluorescence yield, F_m, minus the minimal fluorescence yield, F_o). A grooved sunblock, designed to prevent ambient sunlight from degrading the quality of near-surface fluorescence response of the phytoplankton in the light chamber was mounted facing the emission window of the FRRF light chamber. An intercalibration of the two chambers was performed from data collected during the night casts. An ultraviolet-sterilized Milli-Q water sample was also periodically measured in the dark chamber, to correct for any fluorescence inherent to the instrument itself. All FRRF chambers and light sensor optical heads were cleaned between immersions to prevent fouling.

The estimation of the proportion of functional reaction centers (f) requires dark adaptation of fluorescence yields for up to 30 min (Kolber and Falkowski 1993; Babin et al. 1996). Operational constraints prevented such measurements being made, so f could only be estimated from in situ fluo-

rescence yields that used the dark chamber. This procedure may lead to an underestimation of f and, therefore, P_z, as a result of nonphotochemical quenching processes.

FRRF data processing—The FRRF was operated under the boot protocol, which provides a saturating flash sequence consisting of a series of 100 subsaturation flashlets (each 1-μs duration separated by a 1-μs interval) and a series of 20 relaxation flashlets (each 1-μs duration separated by a 50-μs interval). An autogaining mechanism was not available; therefore, the instrument sensitivity was preset from a knowledge of F_m values at which each gain became saturated and of fluorescence yields from the previous cast. Data were logged to an internal memory card as one set of values averaged from four flash sequences, resulting in a data collection rate of one set of values per 5 s per channel. The CTD was held for 5 min at depths from which the bottle samples were collected in order to obtain an extended series of FRRF measurements (typically 20–30 measurements for each of the light and dark chambers). A reduction in signal to noise ratio for FRRF data from depths shallower than 5–10 m was caused by interference from ambient red light close to the surface.

Data were downloaded from the FRRF in binary format and analyzed by use of a programme supplied by Z.S. Kolber, to provide values of F_o, F_m, the functional absorption cross section of PSII (σ_{PSII}), and the minimum turnover time for electron transport (τ) for both the light and dark chambers. The connectivity parameter (ρ) was fixed at 0.3 for all data analyses. All fluorescence yields are given as instrument units; the photochemical efficiency, F_v/F_m, is nondimensional; τ is given in ms and σ_{PSII} in m^2 mol RCII^{-1}.

$^{14}CO_2$ Primary production measurements—Water samples from two to three depths were taken from each CTD cast for photosynthesis-irradiance (P-E) experiments on the basis of the uptake of ^{14}C in a temperature-controlled photosynthetron (Lewis and Smith 1983), essentially as described by MacIntyre et al. (1996). Illumination in the range 10–1,700 μmol photons m^{-2} s^{-1} was provided by quartz-halogen lamps, filtered through a 2.5-cm layer of water. Irradiance in the manifold was measured with a Biospherical Instruments QSL-101 4π sensor. The cells were held in darkness for up to 30 min between sampling and incubation. The sample was inoculated with 50 μCi mL^{-1} of NaH^{14}CO$_3$ (58 Ci mole^{-1}, Amersham CFA.3). The incubations were terminated after 60 min by adding 50 μl of glutaraldehyde to each aliquot. Residual inorganic carbon was driven off by addition of 250 μl of 6 N HCl and shaking for 60 min, and then the incorporation of ^{14}C was determined by liquid scintillation counting. Total activity of NaH^{14}CO$_3$ was determined on 20-μl aliquots of sample taken directly into scintillation cocktail with 50 μl mL^{-1} β-phenylethylamine. Total inorganic carbon was assumed to equal 2.3 mM. Data were fitted by least-squares, nonlinear regression to the following model:

$$P^{Chl} = \{P_s^{Chl}[1 - \exp(-\alpha^{Chl}E/P_s^{Chl})][\exp(-\beta^{Chl}E/P_s^{Chl})]\} - P_o^{Chl}, \quad (3)$$

where P^{Chl} (g C [g Chl a]$^{-1}$ h^{-1}) is the Chl a–specific photosynthetic rate at irradiance E (μmol photons m^{-2} s^{-1}); P_s^{Chl} is the light-saturated rate of photosynthesis that would be observed in the absence of photoinhibition; α^{Chl} (g C [g Chl a]$^{-1}$ h^{-1}) (μmol photons m^{-2} s^{-1})$^{-1}$ is the initial slope of the P-E curve; β^{Chl} (g C [g Chl a]$^{-1}$ h^{-1}) (μmol photons m^{-2} s^{-1})$^{-1}$ is a photoinhibition parameter; and P_o^{Chl} (g C [g Chl a]$^{-1}$ h^{-1}) is an intercept parameter included to improve the distribution of residuals at low irradiances. The maximum photosynthesis rate, P_m^{Chl}, was calculated as follows:

$$P_m^{Chl} = P_s^{Chl}(\alpha/\alpha + \beta)(\beta/\alpha + \beta)^{\beta/\alpha}. \quad (4)$$

We measured the spectral output of the photosynthetron lamp used for the ^{14}C-uptake experiments with a spectral irradiance photometer standardized against a NAST calibrated lamp. The photosynthetron spectrum was then compared against in situ spectra measured for several depths at each station. The photosynthetron spectrum was measured at 1-nm intervals between 400 and 700 nm, whereas the in situ light was only recorded at seven wavelengths corresponding to the visible wavelengths of SeaWiFS. Therefore, the in situ wavelengths were interpolated nonlinearly, following the shape of a global climatological solar spectrum, to give corresponding in situ irradiance between 400 and 700 nm. The spectral distribution of the photon flux was then normalized such that the total flux between 400 and 700 nm was equal to unity as a means of comparing the light sources (Fig. 1a). The effective Chl a–specific light absorption coefficient (a^*) for the 400–700-nm wavelength interval was then calculated for each light source as follows:

$$a^* = \Sigma[E(\lambda)a^*(\lambda)]/\Sigma[E(\lambda)], \quad (5)$$

where $a^*(\lambda)$ is multiplied by normalized irradiance (E_λ) and then summed for all wavelengths (i.e., 400–700 nm).

The difference in effective absorption coefficient (a^*) between the in situ and photosynthetron light spectra was obtained by dividing the respective rate of light absorption by the irradiance (E, which is equal to 1, since all spectra were normalized). The ratio of mean effective absorption from the photosynthetron light source is 0.53 (Sta. 1), 0.51 (Sta. 2), and 0.41 (Sta. 3) of that measured for the in situ light field. The difference between these two light sources at all three stations was lowest for surface samples, since a greater proportion of red light was observed close to the surface. Therefore, the irradiance (400–700 nm) measured in the photosynthetron is only 0.41–0.53 as effective for photosynthesis as a corresponding value measured in the water column. In order to compensate for these differences in spectral quality, we multiplied the irradiances measured in the photosynthetron by 0.53 (Sta. 1), 0.51 (Sta. 2), and 0.41 (Sta. 3) before calculating values of α^{Chl} and E_k.

A similar correction was applied to the excitation spectra generated from the blue light-emitted diodes (LEDs) of the FRRF (Fig. 1a). Peak excitation is at 478 nm with a 30 nm half bandwidth. The ratio of mean effective absorption from the FRRF is 1.44 (Sta. 1), 1.48 (Sta. 2), and 1.23 (Sta. 3) of that measured for the in situ light field. The FRRF most closely resembles the in situ spectrum in deeper waters, since blue-green light penetrates deepest. Therefore, the effective absorption of light from the FRRF (σ_{PSII}) overestimates that of the in situ light field by a factor of 1.23–1.48, and values of FRRF σ_{PSII} were adjusted accordingly.

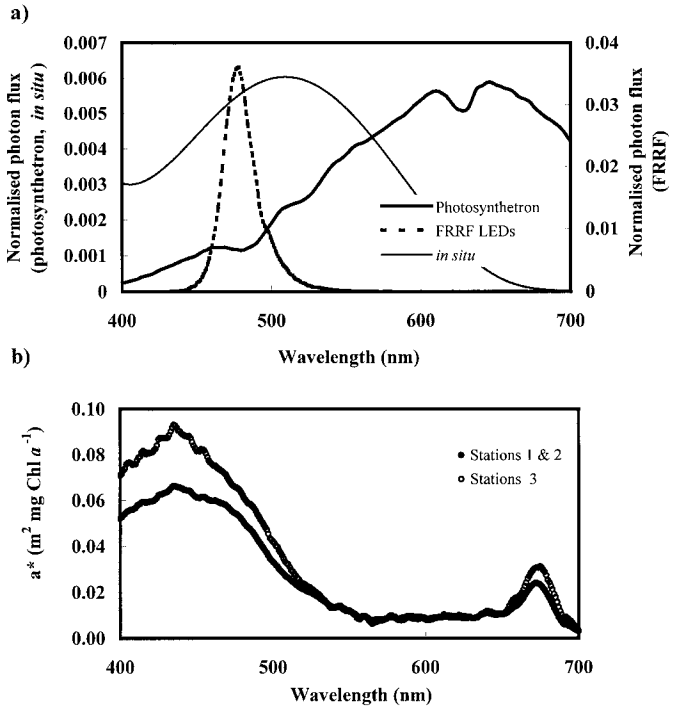

Fig. 1. (a) Normalized (equal area) spectra of photon flux density (μmol photon m^{-2} nm^{-1}), 400–700 nm, measured in the photosynthetron, in situ, and from the FRRF LED. The FRRF LED spectrum was provided by John Atkins, CI. In situ data from seven wavelengths were interpolated by following the shape of a global climatological spectrum. (b) Mean Chl *a*–specific absorption spectrum (*a**, 400–700 nm) for all samples taken at Sta. 1 (n = 9), 2 (n = 14), and 3 (n = 10), irrespective of time of day or depth. The mean *a** at each wavelength is used in Eq. 5 for the calculation of effective absorption under each of the light sources.

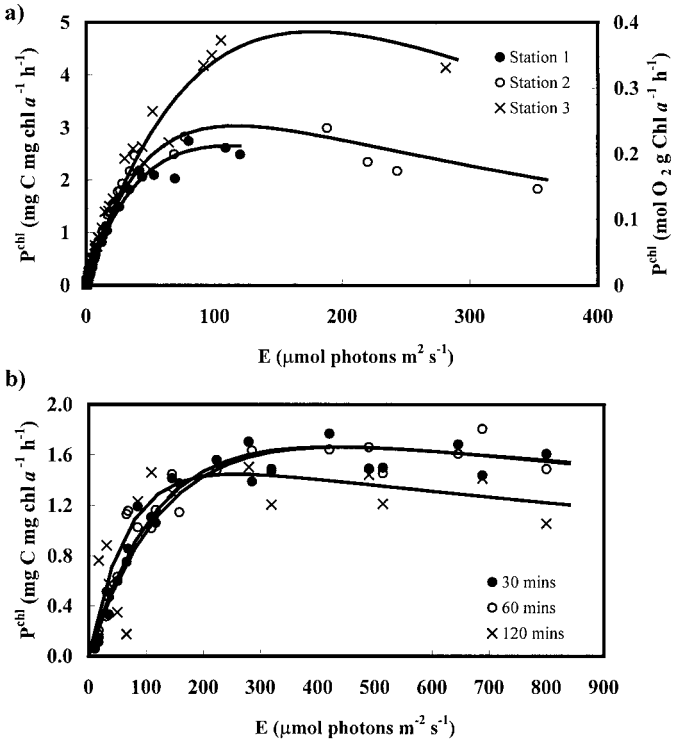

Fig. 2. (a) P-E curves reconstructed from data collected by use of the FRRF at the three sampling sites. P-E curves are fitted with use of least squares, according to Eq. 3. Rates of FRRF instantaneous production [$P(E)$, Eq. 1] are given for both carbon (mg C mg Chl a^{-1} h^{-1}) and oxygen (mmol O_2 mg Chl a^{-1} h^{-1}) and assumes a photosynthetic quotient of 1. (b) P-E curves determined from ^{14}C-uptake experiments. P-E curves are fitted by use of least squares, according to Eq. 3. Data shown are from a 10-m sample from Sta. 2 (40°N) incubated for 30, 60, and 120 min.

O_2 measurements—Dissolved oxygen was determined by use of the ''Shibala'' Winkler spectrophotometric method (Pai et al. 1993). Glass stoppered bottles of 120 ml were flushed and filled with water taken from each of 11 depths for all rosette casts. Winkler chemicals (1 ml $MnCl_2$ 4 H_2O, 600 g L^{-1}, and 2 ml NaOH, 250 g, and KI, 350 g L^{-1}) were added within minutes after sampling by means of dispensers. After shaking and storing of the bottles under water for at least 1 h, 0.8 ml 20N H_2SO_4 was further added. The mixture was stirred with a magnetic stirring bar until the precipitate had dissolved completely. The brown-yellow solution was siphoned to a Hitachi U1000 spectrophotometer equipped with a 1-cm flow-cell (aperture 11 × 4 mm). Absorption was measured at 456 nm on the analog output of the spectrophotometer connecting a four-digit voltmeter (Metex M4650). In this way, we obtained a four-digit readout in the extinction for absorbance, which was necessary in view of the required accuracy. Corrections were made for the seawater color by subtracting the absorption value for untreated seawater and for the effects of the volume of Winkler reagents on measured oxygen concentration. The reproducibility and stability of the method over 5 d and 15 samples was 0.18%.

CTD water sample analyses—Water samples (1 liter) were filtered under positive pressure through Whatman 25-mm GF/F filters, and the filters stored at −80°C prior to analysis for phytoplankton pigments upon return from sea. Total Chl *a* was determined by spectrophotometric analyses after extraction in acetone. Nutrients were measured colorimetrically by use of a Technicon TrAAcs 800 Autoanalyzer.

Absorption spectra were measured on samples filtered onto Whatman GF/F filters, stored at −80°C until analysis, with a Hitachi U-3000 spectrophotometer fitted with a ϕ60 integrating sphere, following the protocol of Tassan and Ferrari (1995). Corrections were made for multiple scattering within the glass-fiber filter by use of a wavelength-independent pathlength amplification factor determined from axenic cultures of *Synechococcus* (strains WH7803 and WH8103). Mean Chl *a*–specific absorption (*a**) spectra collected from the three stations are shown in Fig. 1b.

Modeling diel productivity—A basic model was constructed for calculating primary productivity from the FRRF-derived photosynthetic parameters for comparison with measured changes of water column oxygen concentrations throughout the day. The model uses values of irradiance (E, μmol photons m^{-2} s^{-1}), light absorption, and the photosyn-

Table 1. Summary of the mean (±SE) Chl *a*–specific absorption (a^*, m^2 mg Chl a^{-1}), maximum light saturated photosynthesis (P_m^{chl}, mg C mg Chl a^{-1} h^{-1}), Chl *a*–specific initial slope (α^{Chl} mg C mg Chl a^{-1} h^{-1} [μmol photons m^{-2} s^{-1}]$^{-1}$) and E_k (light saturation parameter, μmol photons m^{-2} s^{-1}) from all samples taken at each of the three sites. Values of a^* were determined from discrete water samples; P_m^{Chl}, α^{Chl}, and E_k were determined from P-E curves after ^{14}C-uptake experiments on discrete water samples and in situ FRRF production estimates. Only one P-E curve was described by the FRRF for each site. The means (±SE) are given for ^{14}C data from shallow (10 m) and deep (30 m Sta. 1 and 2; 40 m, Sta. 3) water samples.

			Sta. 1 (43°N)	Sta. 2 (40°N)	Sta. 3 (37°N)
Absorption coefficient	a^*		0.056 ± 0.005	0.54 ± 0.002	0.064 ± 0.002
FRRF P–E curves	P_s^{Chl}		2.71	3.04	4.78
	P_m^{Chl}		2.40	2.68	4.25
	α^{Chl}		0.045	0.049	0.056
	E_k		60	62	85
^{14}C P–E curves	P_s^{Chl}	shallow	2.28 ± 0.05	1.89 ± 0.26	2.08 ± 0.19
		deep	1.66 ± 0.14	1.57 ± 0.11	1.52 ± 0.39
	P_m^{Chl}	shallow	2.09 ± 0.02	1.69 ± 0.19	1.96 ± 0.21
		deep	1.47 ± 0.16	1.37 ± 0.10	1.32 ± 0.46
	α^{Chl}	shallow	0.022 ± 0.001	0.021 ± 0.002	0.023 ± 0.001
		deep	0.022 ± 0.002	0.022 ± 0.002	0.022 ± 0.009
	E_k	shallow	107 ± 8	92 ± 8	89 ± 3
		deep	79 ± 3	73 ± 5	71 ± 11

thetic parameters determined with the FRRF. The incident irradiance at the sea surface was estimated from the knowledge of time of year and position. The diurnal variability of the incident irradiance was extracted from the uncalibrated ship-mounted PAR sensor and normalized against the highest value. Determination of in situ irradiance incorporates the effects of both reflection and refraction at the sea surface on the underwater light field. The estimates of reflection are dependent on the solar elevation (β) and use a refractive index (water : air) of 1.33 for seawater at ambient temperatures at any wavelength within the PAR spectrum (Kirk 1994). The water surface is assumed to be flat.

In situ irradiance (E) at each time is calculated with respect to depth (z) as the product of the surface irradiance ($E_{0,t}$) and the vertical attenuation coefficient (K_d). Values of K_d were calculated at 10-m intervals from light data collected by a PAR sensor mounted to the CTD frame. An interpolation between these estimates provides a depth-dependent K_d [$K_{d(z)}$] and accounts for vertical differences in the spectral quality of PAR:

$$E_{(z,t)} = E_{(0,t)} \exp[-K_{d(z)}\, z]. \quad (6)$$

The rate of light absorption (a', μmol photons m^{-3} s^{-1}) is given by the product of the irradiance (E) and the Chl *a*–specific absorption coefficient (a^*). Although a spectrum of absorption may be available, a single value of a^* was used for the model, to correspond to the absorption at the peak wavelength of FRRF LED emission (478 nm). In addition, a' includes a characteristic estimate for the Chl *a* concentration ([Chl *a*]):

$$a'_{(z,t)} = E_{(z,t)}\, a^*_{(z,t)}\, [\text{Chl } a]. \quad (7)$$

The rate of primary production is constructed from the product of the rate of light absorption (a') and the photon yield of photosynthesis (ϕ_p, (mol carbon) (mol photons)$^{-1}$). Values of ϕ_p were calculated from FRRF estimates of instantaneous production [$P(E)$] and available measurements of a^* where $\phi_p = P(E)/(a^*E)$. A single relationship was generated between ϕ_p and E from all diel measurements and could then be applied throughout the model:

$$\text{Model } P(E)_{(z,t)} = a'_{(z,t)}\, \phi_p(E). \quad (8)$$

This model was formulated for data from each of the three stations.

Results and discussion

FRRF and ^{14}C measurements of Chl a*–specific photosynthesis*—Rates of photosynthesis were calculated from FRRF data for all three stations (Fig. 2a) by use of Eq. 2. The molar Chl *a* : RCII ratio (i.e., the so-called photosynthetic unit size [PSU]) was assumed to be 300 mol Chl *a* : mol RCII. This value is considered to be typical of cyanobacteria (Falkowski and Kolber 1995), which dominated the phytoplankton at all three stations, as shown by analytical flow cytometry (Vedhuis pers. comm.). $\phi_e(E)$ was calculated from a knowledge of the light saturation parameter, E_k (Kolber and Falkowski 1993). E_k was estimated by fitting observations of F_v/F_m under ambient light (L) to a function that describes the dependence of the photon efficiency of photosynthesis on irradiance ($F_v/F_mL = A[1 - \exp(-E/E_k)]/E$, where $A = [F_v/F_mL(\text{MAX})]/E_k$).

The P-E curves for the three stations (see also Table 1) have reasonably similar light-limited initial slopes (α^{Chl}) of 0.045, 0.049, and 0.056 mg C (mg Chl *a*)$^{-1}$ h^{-1}(μmol photons m^{-2} s^{-1})$^{-1}$ for Sta. 1, 2, and 3, respectively. However, the light-saturated Chl *a*–specific photosynthetic rates (P_m^{Chl}) varied between 2.4 and 4.25 mg C (mg Chl *a*)$^{-1}$ h^{-1}, with the highest value at the southernmost station (Sta. 3: 37N). The changes in P_m^{Chl} suggest differences in the photoacclimation status of the phytoplankton at the three stations, with those at the southernmost station being high-light acclimated and those at the northernmost station low-light acclimated. This hypothesis is consistent with the vertical structure of

the water column, with the deepest wind-mixed layer at the northernmost station.

Photosynthesis-irradiance response curves for carbon-14 uptake (Table 1, Fig. 2b) yielded mean values for the light-limited initial slope of 0.021–0.023 mg C mg Chl a^{-1} h^{-1}(μmol photons m^{-2} s^{-1})$^{-1}$ and mean values for light-saturated photosynthesis (P_m^{Chl}) of 1.3–1.5 mg C mg (Chl a)$^{-1}$ h^{-1}. The values of α^{Chl} are 2–2.5 times lower, and those of P_m^{Chl} are 1.6–2.2 times lower than the corresponding parameter values determined with FRRF. There are several factors that could account for these discrepancies, including an incorrect assumption about the PSU size for FRRF calculations, an error in the estimation of E_k for the FRRF profiles, a failure to account for uncoupling of gross electron transfer (gross oxygen evolution) rates from net carbon-fixation rates in the FRRF calculations, and/or errors in ^{14}C assimilation measurements associated with bottle effects. Although the last possibility cannot be ruled out, the P-E response curves for samples incubated for periods of 30, 60, and 120 min were very similar (Fig. 2b). This result indicates that photosynthetic rates were not time-dependent (at least between 30 and 60 min), suggesting that the incubations were free from artifacts due to sample contamination.

Reconciliation of FRRF and ^{14}C measurements of photosynthetic rate— Estimation of the rate of photosynthesis per unit Chl by use of the FRRF is dependent on assuming an appropriate value for the PSU. Observations on laboratory cultures indicate that PSU size can range from as low as 133 mol Chl a:mol RCII in *Synechococcus* spp. (Barlow and Alberte 1985) to as high as 619 mol Chl a:mol RCII in *Dunaliella tertiolecta* and 609 mol Chl a:mol RCII in *Skeletonema costatum* (Falkowski et al. 1981).

Photosynthetic rates calculated from Eq. 2 vary inversely with PSU size (linearly with n_{PSII}). If we assume values of 420–720 mol Chl a:mol RCII, there is general agreement between α^{Chl} and P_m^{Chl} values determined from the FRRF and ^{14}C methods. However, such an assumption is not warranted, because the phytoplankton at all three stations was dominated by cyanobacteria. Furthermore, indirect estimates of PSU size from measurements of the Chl a–specific light absorption coefficient (Fig. 1b) and σ_{PSII} suggest lower values typical of cyanobacteria. We obtained a mean value for PSU_{RCII} of ~220 mol Chl a mol $RCII^{-1}$, as follows. PSU size is related to σ_{PSII}, a^*, and ϕ_m through the relation $PSU_{O2} = \sigma_{O2}/(\phi_m a^*)$, where PSU_{O2} is the ratio of Chl a to oxygen evolved in a saturating, single turnover flash and σ_{O2} is the cross-section for O_2 evolution (Mauzerall and Greenbaum 1989). We note that $\sigma_{PSII} = \sigma_{O2}$ (units of m^2 $photon^{-1}$), $PSU_{RCII} = PSU_{O2}/4$, and $\phi_m = 0.125$ mol O_2 mol $photons^{-1}$. In order to account for nonfunctional PSII reaction centers, it is also necessary to scale by $1.8/(F_v/F_o)$. Thus, $PSU_{RCII} = (1.8\ \sigma_{PSII})/(0.5F_v/F_o a^*)$, allowing us to calculate values for PSU_{RCII} of 149–304 (mean ± SE, 223 ± 9) for the three stations. These calculations do not help to reconcile the ^{14}C and FRRF results because they suggest that we underestimated, rather than overestimated, photosynthesis with the FRRF. However, a number of uncertainties remain in the estimation of PSU_{RCII}, including the assumption of equal distribution of excitation energy between RCI and RCII within the wavelength band of the FRRF light source, evaluation of the fraction of photochemically active RCIIs from $1.8/(F_v/F_o)$, and measurement of the absorption of light by photosynthetic pigments.

The values of the light saturation parameter (E_k) obtained from ^{14}C-uptake P-E curves exceed those from the FRRF P-E curves by a factor of 1.2–1.8 for Sta. 1 and 2 but are relatively comparable for Sta. 3. However, there is some uncertainty in which values of the E_k determined by ^{14}C assimilation should be used, given the 1.3-fold variation between shallow and deep samples. Given that the FRRF approach determines E_k for the water column, then it would be most appropriate to make the comparison with the highest values of E_k determined by ^{14}C assimilation. The divergence between FRRF and ^{14}C determinations of E_k may, in part, reflect an inaccuracy in the calculation of E_k for FRRF production via the $F_v/F_m L$ versus irradiance curves. If the E_k determined by FRRF is underestimated, then subsequent calculations of the photon yield of electron transfer (ϕ_e) will be underestimated, and the value of P_m^{Chl} will be increased. Conversely, an overestimation of E_k would increase the difference in P_m^{Chl} between the FRRF and ^{14}C techniques. Thus, accurate knowledge of E_k is required for determining the point at which maximal light-saturated photosynthesis occurs in the calculation of FRRF production. Corresponding values of α^{Chl} from the P-E curves are not sensitive to changes in E_k but are instead determined by the accuracy of other variables that contribute to estimates of $P(E)$ via the FRRF.

The FRRF provides a measure of the rate of electron transfer through RCII, which should be proportional to the gross rate of oxygen evolution. The assimilation of ^{14}C is commonly assumed to represent net carbon dioxide fixation even when incubation times are relatively short (≤1 h; Williams et al. 1996). Therefore, the rate of gross oxygen evolution should not be expected to equal that of net carbon fixation. Among the processes that can account for the divergence of gross oxygen evolution from net carbon dioxide assimilation are (1) ''dark'' respiration, (2) the use of reductant generated by photosynthetic electron transfer for reactions other than carbon dioxide fixation, (3) photorespiration, and (4) the Mehler reaction (light-driven oxygen consumption by the photosynthetic electron transfer chain).

Typically, dark respiration can account for a 10% reduction in gross photosynthesis. The use of reductant for processes other than carbon assimilation is accounted for as the photosynthetic quotient (O_2/CO_2). This parameter can vary from 1.4 ± 0.1 when cells are growing with nitrate as the N source to 1.1 ± 0.1 when ammonium is the N source (Laws 1991) but has been reported as high as 2–3 for mixed assemblages of phytoplankton (Williams and Robertson 1991) and in cultures of *Synechoccocus* (Grande et al. 1991). Photorespiration is thought to be unimportant in marine phytoplankton. The Mehler reaction has been reported to account for 50% of gross oxygen evolution at light saturation in *Synechococcus* (Kana 1992).

Thus, a combination of a net-to-gross photosynthesis ratio of 0.9, a photosynthetic quotient of 1.4–2.0, and the Mehler reaction could account for about a 2–3 fold difference between ^{14}C assimilation and gross oxygen evolution. Consistent with this suggestion, Kana (1992) found that light-sat-

urated gross oxygen evolution rates exceeded light-saturated ^{14}C assimilation rates in laboratory cultures of *Synechococcus* by a factor of up to three.

The Mehler reaction is likely to account for uncoupling of gross oxygen evolution from net carbon dioxide fixation at irradiances that exceed E_k but is not thought to be important at low irradiances corresponding to the initial slope region of the P-E curve (Kana 1992). The initial slopes (α^{Chl}) from the FRRF P-E curves exceed those from the ^{14}C curves by a factor of 2.0–2.5 (Table 1). This difference is generally higher than can be explained relative to the importance of CO_2 and other compounds as electron acceptors through the photosynthetic quotient (Falkowski and Raven 1997) and of dark respiration.

Model of in situ productivity based on FRRF parameters— The primary production model takes into account diel changes in incident solar radiation, vertical light attenuation within the water column, light absorption by phytoplankton, and the irradiance-dependence of the photon efficiency of photosynthesis. The output was determined with a depth interval of 2 m (0–40 m) and a time interval of 7 min for data from each of the three sites. Comparisons between the modeled and (FRRF) measured values of both in situ light and rates of production yield highly significant relationships with a gradient close to 1 (Fig. 3). However, the lack of data provided by the FRRF at high light intensities limits the range of these comparisons. A close agreement is also observed when corresponding data of ^{14}C-uptake and FRRF instantaneous rates of Chl *a*–specific production are compared (FRRF P^{Chl} = ^{14}C P^{Chl}*2.166, $r^2 = 0.591$, $n = 22$, $P < 0.001$). Thus, the FRRF yields estimates of production that are approximately two times greater than from the ^{14}C technique.

The mean in situ oxygen concentration, [O_2], was measured throughout the water column at each of the stations (Fig. 4). In situ [O_2] displayed a clear diurnal increase at Sta. 2 and 3. Sta. 1 did not exhibit this pattern but rather showed a general increase in [O_2] throughout the water column between 0800 and 1000 h GMT casts but a decrease during the afternoon casts. There was evidence of advection in the temperature and salinity data for Sta. 1 that precludes a comparison of the FRRF productivity with changes of the in situ O_2. The cumulative production of O_2 from the model is considered for the diel period (Fig. 4). If we assume that the initial (mean) concentration of O_2 in the water column is close to that measured at 0800 h GMT by the Winkler method, the characteristic sigmoid trend of cumulative oxygen production from the model follows that of the measured oxygen content of the water throughout the day but is greater by just over a factor of two at Sta. 2 and 3. This difference reflects an offset between the net oxygen production of the water column, as measured by the Winkler method, and the gross oxygen production from PSII (model/FRRF), which remains throughout the diurnal period. A similar relationship is not observed at Sta. 1 (Fig. 4), perhaps because of water column advective processes.

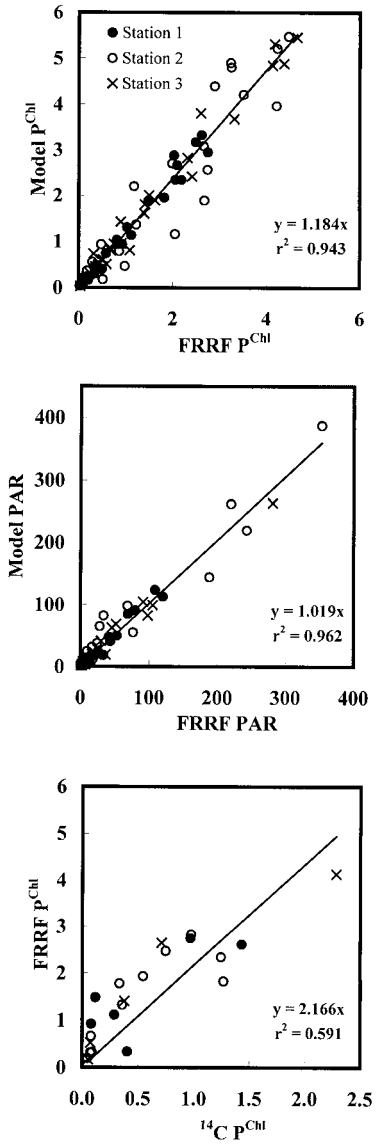

Fig. 3. Relationships between (top) FRRF-measured and modeled Chl *a*–specific rates of in situ instantaneous production [$P^{Chl}(E)$, mg C mg Chl $a^{-1}h^{-1}$] (Sta. 1, $n = 24$; Sta. 2, $n = 24$; Sta. 3, $n = 32$, $P < 0.001$), (middle) measured and modeled in situ irradiance (E, μmol photons m^{-2} s^{-1}) (Sta. 1, $n = 24$; Sta. 2, $n = 24$; Sta. 3, $n = 32$, $P < 0.001$), and (bottom) measured Chl *a*–specific rates of FRRF instantaneous production and ^{14}C uptake for the corresponding depth and time ($n = 22$, $P < 0.001$).

Conclusion

Despite the growing use of fluorescence techniques to provide estimates of production, there are few published comparisons with more ''standard'' techniques, such as ^{14}C uptake. Kolber and Falkowski (1993) obtained a coefficient of determination (r^2) of 0.74 and a slope of 1.06 between paired data from PP fluorescence and ^{14}C-derived (Chl *a*–specific) instantaneous production. Boyd et al. (1997) observed a weaker relationship when comparing P_m^{Chl} from vertical profiles (P-E) using the PP fluorometer and from discretely measured ^{14}C samples; they also observed P_m^{Chl} values from the

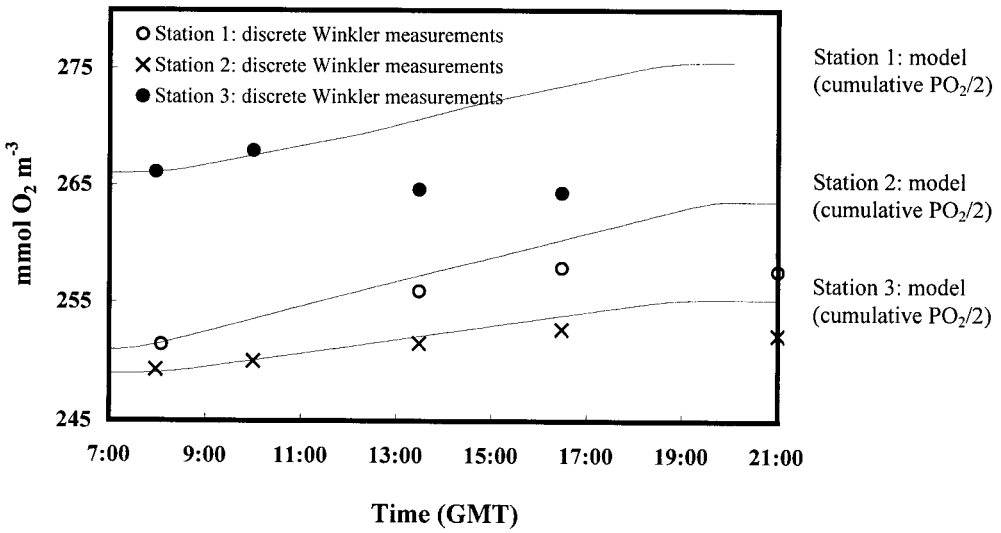

Fig. 4. Relationships between measured oxygen concentrations shown as symbols (Winkler method, mmol O_2 m^{-3}) and modeled cumulative production curves (mmol O_2 m^{-3}). Both measured and modeled data represent the means for 0–40 m at each station. Modeled O_2 production was calculated under the assumption of an initial [O_2] that approximated to the initial mean measured [O_2] (0800 h GMT). The (mean) production is shown for the true modeled O_2 production values (PO_2) divided by 2 and expressed cumulatively. A regression between true modeled O_2 production and measured [O_2] from Sta. 2 (40°N) gives modeled [O_2] = 2.921 × measured [O_2] − 558.4, r^2 = 0.888, n = 4, $0.02 > P > 0.01$. A significant relationship is also observed for data from Sta. 3, where modeled [O_2] = 3.082 × measured [O_2] − 579.5, r^2 = 0.889, n = 5, $P < 0.001$.

PP method that were markedly lower than those from ^{14}C-uptake experiments. However, both these comparisons are limited, since PP methodology involves more assumptions than the FRRF methodology—for example, σ_{PSII} must be assumed to be constant or measured on-deck for the PP technique. Furthermore, these studies used periods of ^{14}C (time integrated) incubation (2–6 h) that were longer than those for the ^{14}C data described here.

Our results show that the FRRF gives in situ estimates of gross O_2 evolution which are positively correlated but significantly higher than those obtained from ^{14}C-uptake methodology. Although this discrepancy can be largely accounted for if the ^{14}C technique approximates net phytoplankton photosynthesis, the possibility remains that a part may reflect oxygen cycling (Kana 1992). Our FRRF versus ^{14}C comparison is consistent with comparisons of gross O_2 production with ^{14}C assimilation (Williams et al. 1983; Grande et al. 1989; Langdon et al. 1995).

References

BABIN, M., A. MOREL, H. CLAUSTRE, A. BRICAUD, Z. KOLBER, AND P. G. FALKOWSKI. 1996. Nitrogen- and irradiance-dependent variations of the maximum photon yield of carbon fixation in eutrophic, mesotrophic and oligotrophic marine systems. Deep-Sea Res. I **43:** 1241–1272.

BARLOW, R. G., AND R. S. ALBERTE. 1985. Photosynthetic characteristics of phycoerythrin-containing marine *Synechococcus* spp. Mar. Biol. **86:** 63–74.

BOYD, P. W., J. AIKEN, AND Z. KOLBER. 1997. Comparison of radiocarbon and fluorescence based (pump and probe) measurements of phytoplankton photosynthetic characteristics in the Northeast Atlantic Ocean. Mar. Ecol. Prog. Ser. **149:** 215–226.

FALKOWSKI, P. G., AND Z. S. KOLBER. 1995. Variations in chlorophyll fluorescence yields in phytoplankton in the worlds oceans. Aust. J. Plant Physiol. **22:** 341–355.

———, T. G. OWENS, A. C. LEY, AND D. C. MAUZERALL. 1981. Effects of growth irradiance levels on the ratio of reaction centres in two species of marine phytoplankton. Plant Physiol. **68:** 969–973.

———, AND J. A. RAVEN. 1997. Aquatic photosynthesis. Blackwell.

GRANDE, K. D., M. L. BENDER, B. IRWIN, AND T. PLATT. 1991. A comparison of net and gross rates of O_2 production as a function of light intensity in some natural phytoplankton populations and in a *Synechococcus* culture. J. Plankton Res. **13:** 153–169.

———, P. J. LE B. WILLIAMS, J. MARRA, D. A. PURDIE, K. HEINEMANN, R. W. EPPLEY, AND M. L. BENDER. 1989. Primary production in the North Pacific Gyre: A comparison of rates determined by the ^{14}C, O_2 concentration and ^{18}O methods. Deep-Sea Res. **36:** 1621–1634.

HU, C., AND K. J. VOSS. 1998. Measurement of solar stimulated fluorescence in natural waters. Limnol. Oceaonogr. **43:** 1198–1206.

KANA, T. M. 1992. Relationship between photosynthetic oxygen cycling and carbon assimilation in *Synechoccocus* WH7803 (Cyanophyta). J. Phycol. **28:** 304–308.

KIRK, J. T. O. 1994. Light and photosynthesis in aquatic ecosystems. Cambridge Univ. Press.

KOLBER, Z. S., AND P. G. FALKOWSKI. 1993. Use of active fluorescence to estimate phytoplankton photosynthesis in situ. Limnol. Oceanogr. **38:** 1646–1665.

———, O. PRASIL, AND P. G. FALKOWSKI. 1998. Measurements of variable chlorophyll fluorescence using fast repetition rate techniques: Defining methodology and experimental protocols. Biochim. Biophys. Acta. **1367:** 88–106.

LANGDON, C., J. MARRA, AND K. KNUDSON. 1995. Measurements of net and gross O_2 production, dark O_2 respiration and ^{14}C assimilation at the Marine Light-Mixed Layers site (59°N, 21°W) in the northeast Atlantic Ocean. J. Geophys. Res **100(C4):** 6645–6653.

LAWS, E. A. 1991. Photosynthetic quotients, new production and net community production. Deep-Sea Res. I **38:** 143–167.

LEWIS, M. R., AND C. J. SMITH. 1983. A small-volume, short-incubation time method for the measurement of photosynthesis as a function of incident irradiance. Mar. Ecol. Prog. Ser. **13:** 99–102.

MACINTYRE, H. L., R. J. GEIDER, AND R. M. MCKAY. 1996. Photosynthesis and regulation of RUBISCO activity in net phytoplankton from Delaware Bay. J. Phycol. **32:** 718–732.

MAUZERALL, D., AND E. GREENBAUM. 1989. The absolute size of a photosynthetic unit. Biochim. Biophys. Acta **974:** 119–140.

PAI, S.-C., G.-C. GONG, AND K.-K. LIU. 1993. Determination of dissolved oxygen in seawater by direct spectrophotometry of total iodine. Mar. Chem. **41:** 343–351.

SAKSHAUG, E., AND OTHERS. 1997. Parameters of photosynthesis: Definitions, theory and interpretation of results. J. Plankton Res. **19:** 1637–1670.

TASSAN, S. AND G. M. FERRARI. 1995. An alternative approach to absorption measurements of aquatic particles retained on filters. Limnol. Oceanogr. **40:** 1358–1368.

WILLIAMS, P. J. LE B., K. R. HEINEMANN, J. MARRA, AND D. A. PURDIE. 1983. Comparison of ^{14}C and O_2 measurements of phytoplankton production in oligotrophic waters. Nature **305:** 49–50.

———, AND J. E. ROBERTSON. 1991. Overall oxygen and carbon dioxide metabolisms: The problem of reconciling observations and calculations of photosynthetic quotients. J.Plankton. Res. (suppl.) **13:** 153–169.

———, AND OTHERS. 1996. Algal ^{14}C and total carbon metabolisms. 2. Experimental observations with the diatom *Skeletonema costatum*. J. Plankton Res. **18:** 1961–1974.

Received: 6 June 2000
Accepted: 18 January 2001
Amended: 26 February 2001